Papers

Polarization in Optical Fibers

IVAN P. KAMINOW, FELLOW, IEEE

(*Invited Paper*)

Abstract—Recent research on fibers with very small or very large birefringence for polarization-dependent applications is reviewed. The nature of random coupling between normal modes of polarization is analyzed and discussed in connection with various applications.

Introduction

In most applications, an optical fiber is a means for transmitting signals in the form of optical power with pulse-code or intensity modulation; the signal is detected by a photodiode that is insensitive to optical polarization or phase. Recently, however, attention has been directed to applications that do depend upon the optical polarization of the wave within a fiber or at its output. Yet, nominally circular fibers do not maintain the input state of polarization for more than a few meters; thus, fibers must be specially designed to maintain polarization.

As in bulk media, the evolution of the polarization state in an optical fiber can be described in terms of a "modal birefringence," i.e., the difference in effective indexes for the orthogonally polarized normal modes. It is our purpose to review the experimental progress in minimizing or maximizing modal birefringence as required for various applications. We will be concerned with fibers that support only one mode in each polarization. We also outline an analysis that describes the nature of random coupling between the two normal modes of a fiber. The effects of modal noise and dispersion in a bimodal fiber are also discussed. Before getting to these topics, however, we review briefly some applications concerned with polarization in fibers.

Applications

A. Small Birefringence

Faraday Effect: The Faraday effect produces a rotation of the plane of polarization about a magnetic field vector. The angle is equal to the product of the Verdet constant, the magnitude of the field, and the optical path length. This rotation of a linear polarization vector can be regarded as being the consequence of a change in phase between the right- and left-hand circular polarization waves that represent the linear polarization wave. In the simplest case, the Faraday effect can only be observed satisfactorily in a fiber medium with perfect circular symmetry about the fiber axis so that the two circular polarized waves are normal modes and, in the absence of a magnetic field, have identical phase velocities. That is, the fiber must have a modal birefringence that is vanishingly small. Then, although the Verdet constant for glass is small, large rotations can be realized because of the long path length available. The current in a conductor can be determined by measuring the magnetic field it induces in a fiber coiled around the conductor or, alternatively, in a straight fiber with the conductor wrapped around it [1], [2].

B. Large Birefringence

1) Interferometers: Nominally circular fibers do not maintain the sense of polarization present at the input for more than a few meters [3], [4] because of polarization-coupling perturbations that are randomly distributed along the length of the fiber, as we describe in greater detail subsequently. However, any device that depends upon the interference of two coherent optical beams, as in homodyne or heterodyne detection, requires that the interacting beams have identical polarizations for efficient operation. If the polarizations of the two beams are 90° apart, complete fading can result. Various fiber optic sensors that depend upon interference have been proposed. In a fiber gyroscope [5]-[7], the phases of two waves traveling in opposite directions in a coil of fiber are compared. In a pressure sensor [8], two separate fibers form the arms of an interferometer bridge; one fiber is subjected to the pressure to be measured and the other serves as reference; the photoelastically induced phase shift provides a measure of the pressure. These applications require fibers that maintain polarization over lengths of several tens to several thousand meters. As we discuss later, large modal birefringence is required for polarization maintaining fibers.

2) Integrated Optics: Many of the waveguide optical switches that have been discussed in connection with inte-

Manuscript received June 9, 1980; revised September 2, 1980.

The author is with Bell Laboratories, Crawford Hill Laboratory, Holmdel, NJ 07733.

0018-9197/81/0100-0015$00.75

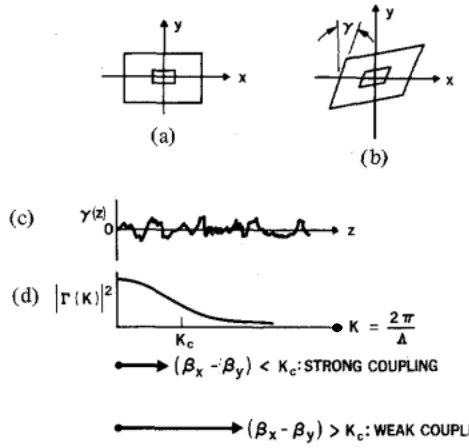

Fig. 1. Polarization coupling by random perturbations: (a) unperturbed cross section; (b) shear perturbation γ; (c) random fluctuations of $\gamma(z)$; (d) power spectrum of fluctuations versus spatial frequency.

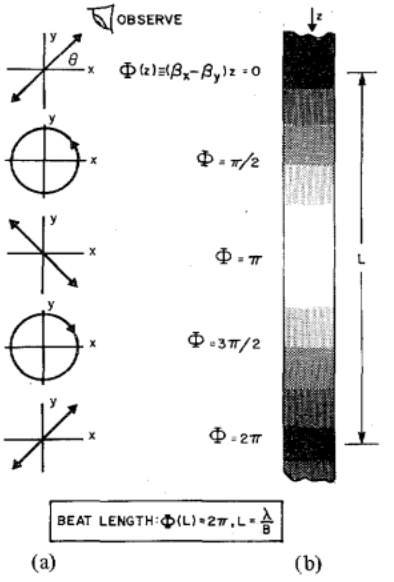

Fig. 2. Beat length: (a) states of polarization versus $\Phi(z)$; (b) scattered intensity observed normal to fiber at angle θ.

grated optical circuits operate effectively only on light that is well polarized [9]. Thus, if such switches are to be utilized at the terminals of long distance communication systems, the fibers employed must maintain polarization over tens of kilometers. If the switches are used in a system linking computer elements within a building, shorter lengths on the order of a kilometer may be suitable. Alternatively, one may employ polarization-insensitive switches [10].

3) Heterodyne Communications: If the two normal modes of polarization were uncoupled over several kilometers in a practical fiber, the information capacity could be doubled by transmitting independent signals on each polarization. Heterodyne detection could then be employed for greater sensitivity.

4) Nonlinear Effects: Optical fiber nonlinear interactions, such as optical Kerr [11] effect, second-harmonic generation, parametric oscillation, and Raman laser oscillation [12], are governed by polarization selection rules. Thus, their efficiency of operation depends upon controlling polarization in the interaction region.

5) Polarization Devices: Several magnetooptic and birefringent optical devices, familiar in bulk form, having been adapted to the fiber geometry. These include a Faraday isolator [13] and a variable compensator [14]. Modal birefringence in the Faraday device is compensated for by utilizing a periodic magnetic field in contrast to the uniform field assumed in the previous section.

Modal Birefringence

So called "single-mode" fibers with nominal circular symmetry about the fiber axis are in fact bimodal in that they can propagate two nearly degenerate modes with orthogonal polarizations; these are the HE_{11}^x- and HE_{11}^y-modes. The principal axes, x and y, are determined by the symmetry elements of the cross section, as in Fig. 1(a). The larger the anisotropy of the cross section, the greater the difference in the propagation constants β_x and β_y for the two normal modes. If the fiber cross section is independent of fiber length z, then the fiber behaves like a birefringent medium with modal birefringence B given by

$$B = (\beta_x - \beta_y)/(2\pi/\lambda) \tag{1}$$

where λ is the optical wavelength. Light polarized along one of the principal axes will retain its polarization for all z. Light polarized at an angle θ with respect to the x-axis will pass through various states of elliptic polarization as the phase retardation

$$\Phi(x) = (\beta_x - \beta_y) z \tag{2}$$

varies with length, provided the two normal mode components maintain phase coherence.

The coherence time for a source with uncorrelated spectral frequency width Δf is $1/\Delta f$. The two normal mode components will be coherent as long as the delay between their transit times is less than the coherence time. The maximum fiber length L_c for which this birefringent coherence holds is approximately [15]

$$L_c \approx c/B\Delta f = \lambda^2/B\Delta\lambda \tag{3}$$

where $\Delta\lambda$ is the wavelength spectral width. For $\lambda = 1\ \mu$m and $\Delta\lambda = 1$ nm, (3) gives $L_c = 250$ km for $B = 4 \times 10^{-9}$ and $L_c = 1$ m for $B = 8 \times 10^{-4}$, which covers the experimental range of B, as noted below. For a single-mode laser with $\Delta f = 1$ MHz, the corresponding values of L_c are 7.5×10^7 km and 3.8×10^3 km, respectively.

For incident linear polarization with $\theta = 45°$ at $z = 0$, the polarization becomes circular for $\Phi = \pi/2$, linear with $\theta = -45°$ for $\Phi = \pi$, circular for $\Phi = 3\pi/2$, and linear with $\theta = 45°$ for $\Phi = 2\pi$, as shown in Fig. 2(a). The length L corresponding to $\Phi(L) = 2\pi$ is called the "beat length,"

$$L = \lambda/B. \tag{4}$$

The beat length can be observed directly by means of dipole (Rayleigh) scattering from the fiber [16]. Since the radiation pattern of a dipole has a null along the dipole axis and a maximum normal to the axis, a fiber viewed along the direction of the incident polarization will exhibit a series of dark and bright bands with period L as shown in Fig. 2(b). It is thus

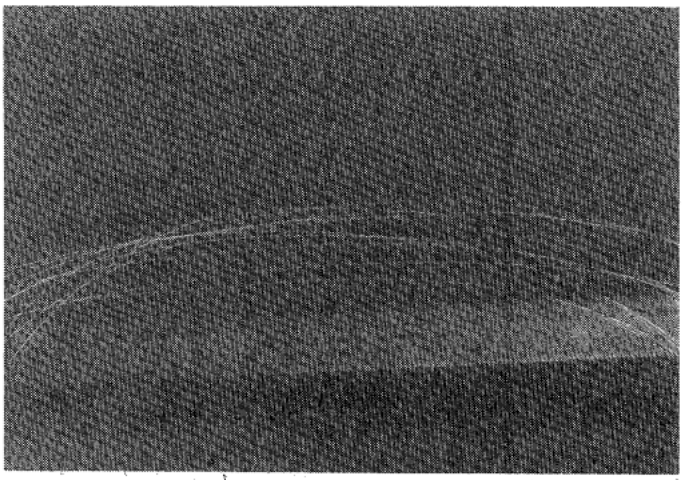

Fig. 3. Polarization beats: L = 1.5 mm at λ = 0.515 μm, $B = 3 \times 10^{-4}$ (see [34]).

possible to determine B from the observed beat length. The beats in the fiber photographed in Fig. 3 have L = 1.5 mm at λ = 0.515 μm; therefore, $B = 3 \times 10^{-4}$.

In a real fiber, perturbations along the fiber can couple energy from one normal mode to the other. These perturbations may be variations in geometry, composition, or strain. They can originate in the preform, in the drawing apparatus, in the cabling, or simply in bends and twists of the fiber. If the perturbations could be determined quantitatively along the length of each fiber, the state of the output polarization could be calculated directly [17]. However, since this information is usually not available, we take the perturbation to be a random function of z. Perturbations having principal axes not coincident with the unperturbed fiber axes will serve to couple energy between the normal modes. The coupling strength is greatest when the perturbation axes make an angle of 45° with the fiber axes. A shear strain that will couple x and y polarizations is illustrated in Fig. 1(b). The coupling strength is, roughly speaking, a function of the ratio of the birefringence of the perturbation to the birefringence of the unperturbed fiber.

Light can be completely coupled from one polarization mode to the other only if the perturbation has period Λ, such that

$$|\beta_x - \beta_y| = K \pm \Delta K \tag{5}$$

where $K = 2\pi/\Lambda$ is the spatial frequency of the perturbation in the z-direction and $\Delta K = \pi/l$, with l the length of fiber. In general, the perturbation $\gamma(z)$ will be a random function of z with average value $\langle\gamma(z)\rangle = 0$, as shown in Fig. 1(c). The random function describing each length of fiber depends upon its history. Deterministic periodic perturbations such as those due to the pitch of lead screws and natural resonances in the drawing process or the lay of fibers in a cable may also be present. The Fourier transform of the correlation function $\gamma(z)$ yields the power spectrum $|\Gamma(K)|^2$ as a function of spatial frequency.

No statistical data are available on the nature of $|\Gamma(K)|^2$ for polarization-coupling perturbations. However, measurements of fluctuations in fiber diameter [18] with z yield a power spectrum with a low-pass filter characteristic as illustrated schematically in Fig. 1(d). Typically, the power spectrum at Λ = 1 mm is −40 dB below the value at $\Lambda \to \infty$. Thermodynamic considerations also lead to the conclusion that the power spectrum of fluctuations produced in the fiber drawing process must approach cutoff for Λ less than a critical value. In addition, the observation that scattering losses are negligible in a good fiber indicates that significant fluctuations in fiber properties must have periods greater than about 1 mm since coupling between guided and radiation modes would require a period $\Lambda < \lambda/\Delta n \approx 1$ mm, when $\lambda = 1$ μm and the core-cladding index difference $\Delta n \approx 10^{-3}$. Thus, we expect $|\Gamma(K)|^2$ to have a low-pass shape similar to that shown in Fig. 1(d).

If we define a cutoff spatial frequency K_c such that

$$\frac{|\Gamma(K_c)|^2}{|\Gamma(0)|^2} = 10^{-q} \tag{6}$$

where q is an integer, say 4, then the transfer of power between polarizations should be small for

$$|\beta_x - \beta_y| \gg K_c \tag{7}$$

or, in terms of the beat length (4) and cutoff period $\Lambda_c = 2\pi/K_c$, the power transfer should be small for

$$L \ll \Lambda_c. \tag{8}$$

Based on the estimate above of $\Lambda_c \approx 1$ mm, (8) requires $B \gg 10^{-3}$. Since $|\Gamma(K)|^2$ probably does not vanish identically even for $K \gg K_c$, we can always expect some coupling for long fibers. A more rigorous treatment of polarization coupling is given in a later section.

The design of polarization maintaining fiber should be concerned with two aspects of the problem: 1) maximize the modal birefringence B or, equivalently, minimize the beat length L; 2) minimize the strength of polarization coupling perturbations with period $\Lambda = \lambda/B$, i.e., increase Λ_c. Efforts to increase B by introducing geometrical anisotropy or strain birefringence in the fiber cross section will be described later. On the other hand, very little is known at present about the nature, sources, or statistics of polarization-coupling perturbations. Any effects that alter the principal axes must be considered; these include eccentricities in the preform or the drawing apparatus, fluctuations in drawing speed and temperature, mechanical resonances near the molten preform tip, twisting and bending of the fiber, transverse strains due to jacketing, and cabling, and axial strains due to differential thermal expansion of components of the fiber. Thus, research along the second path 2) is needed in order to realize the ultimate in polarization maintaining fibers.

Small Birefringence

Modal birefringence B can be separated into two components: a geometrical contribution G and an effective material birefringence M due to strain

$$B = M + G. \tag{9}$$

The M and G contributions may have either the same or opposite signs. The effective M is an average, weighted by the

square of the modal wave function, over the actual material birefringences of the core and cladding glasses.

These strain and geometrical effects on polarization in optical fibers were first discussed by Snitzer and Osterberg [19]. Ramaswamy [20] noted that, for a small core cladding index difference, Δn, strain birefringence could make the dominant contribution to B.

Various expressions have been proposed for G but for small ellipticity e, a good approximation is [21], [22]

$$G \approx C \cdot \frac{\lambda}{d} e^2 \Delta^{3/2} = \hat{C} \cdot e^2 \Delta^2 \tag{10}$$

where d is the mean core diameter

$$\Delta = \Delta n/n \tag{11}$$

$$e = [1 - (d_y/d_x)^2]^{1/2} \tag{12}$$

and d_y and d_x are the minor and major core diameters, respectively. The constant C depends upon the fiber V value [see (15)] and has its maximum value ($\sim$0.06) at $V \approx 2.5$, near the cutoff for the first higher order mode; and $\hat{C} = 2\sqrt{2}\,\pi C/V$.

It is clear from (9) and (10) that in order to obtain $B \to 0$ for use in Faraday effect or circular polarization applications M, e and Δ must be small and d/λ large (while still maintaining fundamental mode behavior). Very low birefringence fibers have been obtained [23], [24] in this way. The lowest value reported [24] is $B = 4.5 \times 10^{-9}$ (L = 140 m at $\lambda = 0.63$ μm) in a fiber for which the thermal expansion coefficients for core and cladding glasses were matched to minimize M. Extreme care must be taken in jacketing and winding these fibers in order not to introduce bends or twists that contribute to birefringence [23]. Strain birefringence can be reduced almost completely by employing a liquid core fiber [25]; thus only the strain in the cladding contributes to M.

Large Birefringence

For applications that require a well-defined linear polarization, it is advantageous to maximize B by maximizing M, G, or both M and G. For large eccentricity, the approximate relation

$$G = C'(\Delta n)^2 \tag{13}$$

holds with C', a coefficient that depends upon the eccentricity and effective V-value. In one approach [26], the maximum value of C', which occurs for a slab geometry ($e = 1$), is about 0.4 for a single-mode fiber. In another approximation [20], [27],

$$C' = [(4\pi)^2/2n]\ [(V_y + 2)^{-3} - (V_x + 2)^{-3}] \tag{14}$$

where the V values are

$$V_i = d_i k (2n\Delta n)^{1/2}, \quad i = x, y \tag{15}$$

and

$$k = 2\pi/\lambda. \tag{16}$$

The range of validity of (14) is discussed in [20]. The maximum value of C' obtained for a fundamental-mode design is about unity. By "fundamental mode," we mean that the wave function does not exhibit a null in either the x- or y-directions, i.e., $V_x < V_o$, where V_o gives the cut off for the next higher order mode and is roughly $V_o \approx 4$ [27]-[29]. Thus, at $\lambda = 1$ μm with $e = \frac{2}{3}$, for $d_x = 5$ μm, we require $\Delta n < 5 \times 10^{-3}$ for fundamental-mode operation and calculate from (10) $G \leqslant 3 \times 10^{-5}$; but for $d_x = 1$ μm we require $\Delta n < 0.14$ and calculate $G \leqslant 2 \times 10^{-2}$. Hence, it is possible to obtain large G, in principle, but at the expense of very small core dimensions, which are difficult to manage in practice.

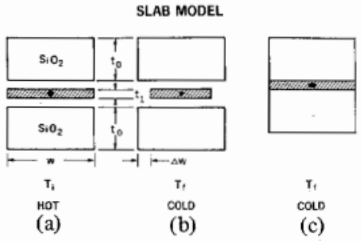

Fig. 4. Slab model: (a) and (b) slabs free; (c) slabs joined.

Experimentally, a beat length $L = 0.75$ mm at $\lambda = 0.63$ μm ($B = 8 \times 10^{-4}$) has been reported by Dyott *et al.* [25] for a fiber with heavily doped core (Ge + P) having $\Delta n = 0.065$ with $e = 0.6$. The fiber was collapsed elliptically with core dimensions 0.85 μm by 2.14 μm. No attenuation measurements were reported. All of the modal birefringence was attributed to G, although it seems reasonable (as noted below) that some M contribution may also be present. It can be shown [27] that M and G, as given in (9), are both positive, and therefore, would add to give the observed B.

In an earlier experiment, elliptical core [20] or cladding [30]-[32] geometries were achieved in borosilicate fibers by collapsing the preform under vacuum or by grinding flats on the preform before collapse, respectively. Because of the smaller Δn ($\approx 10^{-3}$), the G values were quite small and most of the observed B ($\approx 10^{-5}$) was attributed to strain effects. Although Dyott [25], [26] did not indicate the details of his elliptical fiber, one may surmise that it resembles these borosilicate fibers in terms of strain effects.

Transverse strain birefringence can be produced intentionally by differential thermal contraction as the fiber is drawn from a preform in order to maximize B. The maximum effect is obtained in a slab geometry [27] as illustrated in Fig. 4. Consider a very thin slab of heavily doped silica with thickness t_1 sandwiched between two thick slabs of silica of thickness t_0 with $t_0 >> t_1$. If each slab has the same width w at some high temperature T_i and if the slabs are free to move, then at a lower temperature T_f the inner slab will have a lesser width by an amount Δw because the thermal expansion coefficient α_1 for doped silica is greater than the coefficient α_0 for pure silica, for most common dopants. On the other hand, if the slabs are attached at their interfaces at T_i in a preform and are drawn into a fiber at T_f (room temperature), the inner slab will be under tension in the x-direction, the plane of the slabs, with strain

$$S_x = (\alpha_0 - \alpha_1)(T_i - T_f). \tag{17}$$

Since the outer slabs are thick, they are rigid and assume their strain-free equilibrium dimensions. There is no constraint present in the y-direction so that $S_y = 0$ for all slabs. (The

strain in the inner slab in the z-direction will be the same as S_x; $S_x = S_z$.)

The outer slabs serve as the strain inducing jacket, the doped-inner slab as the cladding, and a more heavily doped region in that slab as the guiding core. We can calculate the strain birefringence b in core and cladding glasses, and estimate the effective modal birefringence M by introducing certain simplifying assumptions [27]. The expansion coefficient α_1 is approximately a linear function of dopant concentration. The initial temperature to be used in (17) is roughly the glass softening temperature. With suitable estimates for these parameters for realizable concentrations of typical dopants, the values calculated [27] for glasses with 10 M percent B_2O_3, or 25 M percent GeO_2, or 14 M percent P_2O_5, respectively, are

$$S_x = +7.6 \times 10^{-4}, \quad +16.3 \times 10^{-4}, \quad +20.8 \times 10^{-4} \tag{18}$$

$$b = (n_x - n_y) = +2 \times 10^{-4}, \quad +4 \times 10^{-4}, \quad +5 \times 10^{-4} \tag{19}$$

where b is obtained from S_x via the photoelastic constant. The birefringence b in (19) corresponds to the core doping concentration, the birefringence in the more lightly doped cladding would be somewhat less. Both S_x and b are proportional to doping concentration and could be increased beyond (18) and (19) if higher concentrations could be realized. The tensile strain values in (18) are already close to the elastic limits for glass. The material birefringence b can be measured directly on slices of fiber by means of a polarizing microscope [27].

The effective modal strain birefringence M would be given by an average of material birefringence b over core and cladding with the wave function squared as weighting factor. Far from cutoff, we have to good approximation

$$M \approx b \tag{20}$$

with b the material birefringence in the core glass. Thus, at $\lambda = 0.5$ μm, the beat lengths corresponding to (19) are

$$L = 2.5, 1.25, 1 \text{ mm}. \tag{21}$$

As a practical matter, it is useful to allow the jacket to surround the cladding as in Fig. 5(b). The strain birefringence is not significantly reduced as long as the thickness of the added wall $2w'$ is much less than w, so that S_y in the inner slab is negligible.

On the other hand, if w' is large, $2w' >> w$, S_y and S_x should be equal so that $b = 0$. Nevertheless, experimental fibers with an elliptical core and/or cladding surrounded by a thick jacket do exhibit strain birefringence [31]. The proposed reason is that the materials flow rather than yield to elastic strain as we have assumed above. The silica hardens at a temperature well above that for the heavily doped glasses. When M was plotted against ellipticity e for a fiber with a round silica core, elliptical borosilicate cladding, and thick surrounding silica jacket, it was found that $M \approx b$ approached 2×10^{-4} as e approached 1, in agreement with (19).

Preforms with the ideal slab geometry are difficult to prepare with high purity glasses. However, strain birefringence approximating that of the slab geometry can be intentionally introduced by the "exposed cladding" technique [33]. One starts with a circular preform containing core, cladding, and thick jacket. Then part of the jacket is removed to asymmetrically expose, or nearly expose, the cladding. The technique was first applied to a borosilicate fiber [33] and later applied to a germanosilicate fiber [34] as illustrated in Fig. 5. The round preform, with about 25 percent GeO_2 in the core, is cut as indicated in Fig. 5(a). When the fiber is drawn, surface tension minimizes the perimeter and produces the cross section photographed in Fig. 5(c), which is seen to be a good approximation to the ideal geometry in Fig. 5(b). Based on the beat length $L = 1.5$ mm at $\lambda = 0.515$ μm for this fiber [34], as shown in Fig. 3, $B \approx M = 3.2 \times 10^{-4}$, which is in reasonable agreement with (19) when uncertainties in the calculation and experiment are considered. The material birefringences b measured in the core and cladding, respectively, using a polarizing microscope were $+3.3 \times 10^{-4}$ and $+2.1 \times 10^{-4}$. The geometrical contribution to B should be relatively small and is neglected here.

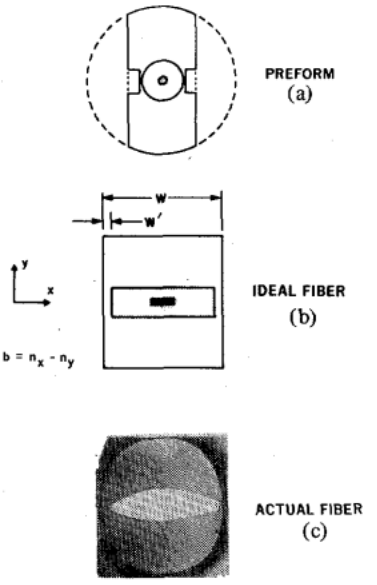

Fig. 5. Exposed cladding method (from [34]): (a) cutting the preform; (b) ideal, slab-like cross section; (c) photograph of fibers.

If a normal mode with polarization x is excited at the input of a fiber of length l and the output powers in the two normal modes are P_x and P_y, then the extinction coefficient η is defined as

$$\eta = P_y/P_x. \tag{22}$$

For $l = 10$ m at $\lambda = 0.515$ μm, the measured η for the above fiber was less than 10^{-3}. It was difficult to measure very small η because of energy guided in the cladding. The fiber attenuation was also large (>100 dB/km), which limited the length that could be studied [34].

Analysis of Random Polarization Coupling

We would like to calculate the powers P_x and P_y as functions of fiber length z due to the random perturbations that couple the two polarizations. Since every length of fiber is different and may vary with time or environment, the best we can do is to compute an ensemble average over all fiber lengths:

$$\langle \eta \rangle = \langle P_y \rangle / \langle P_x \rangle. \tag{23}$$

The problem of mode coupling by random perturbations has been treated by Marcuse [35], [36]. Adapting his analysis to polarization modes, we find

$$\langle P_x \rangle = e^{-hz} \cosh hz \tag{24}$$

$$\langle P_y \rangle = e^{-hz} \sinh hz \tag{25}$$

$$\langle \eta \rangle = \tanh hz \tag{26}$$

for $P_x(0) = 1$ and $P_y(0) = 0$.

The coupling parameter h is obtained from [36]

$$f_{xy}(z) = \frac{\omega \epsilon_o}{4iQ} \int\int \boldsymbol{E}_x^* \cdot \gamma(z) \cdot \boldsymbol{E}_y \, dx \, dy \tag{27}$$

with

$$Q = \frac{1}{2} \epsilon_o c \int\int |E_x|^2 \, dx \, dy \tag{28}$$

where $\gamma(z) \equiv (\epsilon - \bar{\epsilon})$ is a tensor random quantity that represents the small deviations of the dielectric tensor $\epsilon(x, y)$ from the unperturbed dielectric tensor $\bar{\epsilon}$ as a function of z. Only off-diagonal elements $\gamma_{xy}(z)$ give nonvanishing coupling.

Any strains or geometrical variations that have principal axes not coincident with x, y will contribute to γ_{xy}. These distortions may be introduced during manufacture or during operation as the result of bends, twists, stresses, or temperature changes. Strains introduced by a bend produce a birefringence with axes in the plane of the bend and normal to it [37]. Strains introduced by a twist rotate the polarization through an angle about 0.07 times the twist angle [38]. Lateral strains produced by external stresses introduce differential birefringence components along and normal to the stress [39].

The optical fields $\boldsymbol{E}_x$ and $\boldsymbol{E}_y$ for the fundamental HE_{11}^x- and HE_{11}^y-modes have similar functional forms but with x and y interchanged. Thus, (27) and (29) give

$$f_{xy}(z) = (k/2i) \, \gamma_{xy}(z) \tag{29}$$

where $i = \sqrt{-1}$. On the average, the perturbation vanishes:

$$\langle \gamma_{xy}(z) \rangle = 0. \tag{30}$$

The autocorrelation function of the random perturbations is

$$R(u) = \langle \gamma_{xy}(z) \, \gamma_{xy}(z - u) \rangle \tag{31}$$

and the power spectrum is

$$\langle |\Gamma(K)|^2 \rangle = \int_{-\infty}^{\infty} R(u) \exp(-iKu) \, du. \tag{32}$$

Thus [35],

$$h = (k^2/4) \langle |\Gamma(Bk)|^2 \rangle \tag{33}$$

where $Bk = (\beta_x - \beta_y)$ is the difference in propagation constants for the coupled modes.

It is clear from (26) that $\langle \eta \rangle \to 1$ as $z \to \infty$, unless h is identically zero. In most cases of practical interest, $hz \ll 1$, so that

$$\langle \eta \rangle \approx hz. \tag{34}$$

For the 10 m long fiber with $\eta < 10^{-3}$ that was mentioned in the previous section, we estimate $h < 10^{-4}$ m^{-1}, and, for a fiber having the statistical properties of this 10 m section, we calculate from (34) $\eta < 10^{-1}$ for $l = 1$ km.

It is evident from (33) that h can be reduced by reducing $|\Gamma(K)|^2$ at $K = Bk$ either by reducing the power spectrum function or, assuming $|\Gamma(K)|^2$ decreases monotonically with increasing K, by increasing B. A direct experimental study of $|\Gamma(K)|^2$ on a scale less than $\Lambda = 1$ mm would appear to be quite tedious and difficult. However, one could make reasonable changes in fiber preparation and measure h in order to note improvements. One could also prepare similar fibers with different values of B in order to map $|\Gamma(K)|^2$.

Modal Noise in Bimodal Fibers

The problem of modal noise in multimode fibers has been discussed by Epworth [40]. The relative delays between modes may vary with time due to thermal drifts in the wavelength of the laser source, or to thermal or mechanical phase shifts in the fiber. With a coherent source, the interference (speckle) pattern at the output of the fiber will fluctuate. However, if the fiber is lossless, the total output power will be constant. On the other hand, if an aperture (such as a misaligned splice) or mode-selective loss (such as micro- or macrobending) is present, the total output power will fluctuate. The amplitude of fluctuations, normalized to the average power, will increase with a decrease in number of modes propagated, other things being equal.

The worst case occurs in a bimodal fiber where complete fading can occur as the phase shift between the modes varies between 0 and 180°. A "single-mode" fiber that is propagating two modes with orthogonal polarizations is a case in point. Then any polarization-sensitive loss will give rise to modal noise, or fading.

A beam splitter used as a monitor is an example of a polarization-sensitive device that should be avoided. However, because of the paraxial nature of the fundamental-mode fiber, other types of perturbations, such as bending loss in a coiled fiber, nonnormal splices, or directional coupler taps are not expected to introduce substantial polarization-dependent absorption. Nevertheless, the designer of a nominally circular "single-mode" fiber system should make a quantitative estimate of this noise source or avoid introducing polarization-sensitive loss mechanisms.

Dispersion in Birefringent Fibers

In a typical fiber system, special care is not taken to excite just one of the normal modes of polarization and the light travels in both modes of the fiber. The delay between the two orthogonally polarized waves is

$$\tau = (l/c) \left(B + k \frac{dB}{dk} \right). \tag{35}$$

The second term may be neglected when the modes are far from cut-off or when $B \approx M$ with G negligible. In this case, the pulse-spreading of an impulse traveling in both polarizations is given by $(\tau/l) = 1$ ps/km ($\approx 500\, G$ Hz · km) for $B = 3 \times 10^{-7}$, corresponding to a nominally circular fiber, and

$(\tau/l) = 1$ ns/km ($\approx$500 MHz · km) for $B = 3 \times 10^{-4}$. In the former example, B will not limit the performance of systems with bit-rates less than 1 Gbit/s and $l < 100$ km, but in the latter example B will introduce a modal dispersion limit unless all the energy is propagated in one mode.

If G is not negligible and the fiber is operated near cutoff, the second term in (35) must be taken into account. The two terms may have opposite signs so that $\tau(V)$ is maximum at $V = 1.2$ and vanishes at $V = 2.5$ [21], [22], [26]. The maximum value is approximately

$$\tau(1.2) \approx 2nle\Delta^2/c. \tag{36}$$

For $e = 0.1$ and $\Delta = 0.06$, (36) gives a polarization dispersion of 40 ps/km or 25 GHz · km. Polarization dispersion of this magnitude is the limiting bandwidth constraint for slightly elliptical single-mode fibers operating near the minimum material dispersion wavelength at 1.3 μm or near the waveguide compensated minimum at 1.5 μm [41]. More complete calculations [41] also show that the core ellipticity must be less than 2.5 percent in order to realize a bandwidth of 100 GHz km at 1.15 μm.

The polarization-mode dispersion has been measured [15] in a nominally circular fiber and found to be in agreement with (35). Compensation of the dispersion in a short length of fiber by a double twist was also demonstrated. It was noted that for random coupling between the polarizations, the dispersion delay would be proportional to $l^{1/2}$, as in multimode fibers with mode coupling. The pulse spreading in the presence of mode coupling is proportional to $(ll_c)^{1/2}$, where l_c is a characteristic coupling length [42]. In the case of (26), $l_c \approx h^{-1}$. Thus, large h would reduce modal dispersion well below the value calculated in (35).

Conclusions

Interest in the utilization of polarization effects in fibers is continuing to grow. A number of valuable and elegant devices have already been proposed and demonstrated; and we should expect others.

Practical application of these devices call for low-loss fibers that possess either very low modal birefringence or very large birefringence with very small mode coupling perturbations. Virtually nothing has been done to study or minimize these perturbations. Although the problem is difficult to attack, it is essential for the realization of polarization maintaining fibers.

Fibers with modal birefringence B as small as 4.5×10^{-9}, with beat length $L = 140$ m at $\lambda = 0.63$ μm, have been demonstrated. These fibers appear to be suitable for Faraday effect devices requiring relatively short lengths in a well-controlled environment.

Fibers, with B as large as 8×10^{-4}, with $L = 0.75$ mm at $\lambda = 0.63$ μm, have already been demonstrated. These fibers may be suitable for sensor and other applications requiring short lengths. However, unless the cut off period Λ_c for coupling perturbations can be increased well beyond L, it is not likely that polarization can be satisfactorily maintained over lengths much greater than 1 km.

Although losses appear to be large in the large B fibers at present, high-loss may not be intrinsic, even with the high doping concentrations required. Nevertheless, recent measurements indicate Rayleigh scattering can introduce losses in excess of 2 dB/km at 1.5 μm for fibers heavily doped with germanium [43]. New geometries, fabrication conditions, or dopants may soon provide low-loss, polarization-maintaining fibers.

References

[1] H. Harms, A. Papp, and K. Kempter, "Magnetooptical properties of index-gradient optical fibers," *Appl. Opt.*, vol. 15, pp. 799–801, 1976.

[2] A. M. Smith, "Polarization and magnetooptical properties of single-mode optical fibers," *Appl. Opt.*, vol. 17, pp. 52–56, 1978.

[3] L. G. Cohen, "Measured attenuation and depolarization of light transmitted along glass fibers," *Bell Syst. Tech. J.*, vol. 50, pp. 23–42, 1971.

[4] F. P. Kapron, N. F. Borelli, and D. B. Keck, "Birefringence in dielectric optical waveguides," *IEEE J. Quantum Electron.*, vol. QE-8, pp. 222–225, 1972.

[5] V. Vali and R. W. Shorthill, "Ring interferometer 950 m. long," *Appl. Opt.*, vol. 16, pp. 290–291, 1977.

[6] S. Ezekiel and S. R. Balsamao, "Passive ring resonator laser gyroscope," *Appl. Phys. Lett.*, vol. 30, pp. 478–480, 1977.

[7] R. Ulrich and M. Johnson, "Fiber-ring interferometer: Polarization analysis," *Opt. Lett.*, vol. 4, pp. 152–154, 1979.

[8] G. B. Hocker, "Fiber-optic sensing of pressure and temperature," *Appl. Opt.*, vol. 18, pp. 1445–1448, 1979.

[9] R. A. Steinberg and T. G. Giallorenzi, "Performance limitations imposed on optical waveguide switches and modulators by polarization," *Appl. Opt.*, vol. 15, pp. 2440–2453, 1976.

[10] R. C. Alferness, "Polarization-independent optical directional coupler switch using weighted coupling," *Appl. Phys. Lett.*, vol. 35, pp. 148–750, 1979; W. K. Burns, T. G. Giallorenzi, R. P. Moeller, and E. J. West, "Interferometric waveguide modulator with polarization-independent operation," *Appl. Phys. Lett.*, vol. 33, pp. 944–947, 1978.

[11] R. H. Stolen and A. Ashkin, "Optical communication effect in glass waveguide," *Appl. Phys. Lett.*, vol. 22, pp. 294–296, 1973.

[12] R. H. Stolen, "Polarization effects in fiber Raman and Brillouin lasers," *IEEE J. Quantum Electron.*, vol. QE-15, pp. 1157–1160, 1979.

[13] R. H. Stolen and E. H. Turner, "Faraday rotation in highly birefringent optical fibers," *Appl. Opt.*, vol. 19, pp. 842–845, 1980.

[14] R. Ulrich, "Polarization stabilization on a single-mode fiber," *Appl. Phys. Lett.*, vol. 35, pp. 840–842, 1979.

[15] S. C. Rashleigh and R. Ulrich, "Polarization mode dispersion in single-mode fibers," *Opt. Lett.*, vol. 3, pp. 60–62, 1978.

[16] A. Papp and H. Harms, "Polarization optics of index-gradient optical waveguide fibers," *Appl. Opt.*, vol. 14, pp. 2406–2411, 1975.

[17] A. Simon and R. Ulrich, "Evolution of polarization along a single-mode fiber," *Appl. Phys. Lett.*, vol. 31, pp. 517–520, 1977.

[18] P. H. Krawarik and L. S. Watkins, "Fiber geometry specifications and its relation to measured fiber statistics," *Appl. Opt.*, vol. 17, pp. 3984–3989, 1978.

[19] E. Snitzer and H. Osterberg, "Observed dielectric waveguide modes in the visible spectrum," *J. Opt. Soc. Amer.*, vol. 51, pp. 499–505, 1961.

[20] V. Ramaswamy and W. S. French, "Influence of noncircular core on the polarization performance of single mode fibers," *Electron. Lett.*, vol. 14, pp. 143–144, 1978; V. Ramaswamy, W. G. French, and R. D. Standley, "Polarization characteristics of noncircular core single-mode fibers," *Appl. Opt.*, vol. 17, pp. 3014–3017, 1978; V. Ramaswamy, R. D. Standley, D. Sze, and E. G. French, "Polarization effects in short length, single-mode fibers," *Bell Syst. Tech. J.*, vol. 57, pp. 635–651, 1978.

[21] J. D. Love, R. A. Sammut, and A. W. Snyder, "Birefringence in elliptically deformed fibres," *Electron. Lett.*, vol. 15, pp. 615–616, 1979.

[22] D. L. A. Tjaden, "Birefringence in single-mode optical fibre due to core ellipticity," *Philips J. Res.*, vol. 33, pp. 254–263, 1978.

[23] H. Schneider, H. Harms, A. Papp, and H. Aulich, "Low-birefringence single-mode optical fibers: Preparation and polarization characteristics," *Appl. Opt.*, vol. 17, pp. 3035–3037, 1978.

[24] S. R. Norman, D. N. Payne, M. J. Adams, and A. M. Smith, "Fabrication of single-mode fibers exhibiting extremely low polarization birefringence," *Electron. Lett.*, vol. 15, pp. 309–310, 1979.
[25] A. Papp and H. Harms, "Polarization optics of liquid-core optical fibers," *Appl. Opt.*, vol. 16, pp. 1315–1319, 1977.
[26] R. B. Dyott, J. R. Cozens, and D. G. Morris, "Preservation of polarization in optical-fiber waveguides with elliptical cores," *Electron. Lett.*, vol. 15, pp. 380–382, 1979.
[27] I. P. Kaminow and V. Ramaswamy, "Single-polarization optical fibers: Slab model," *Appl. Phys. Lett.*, vol. 34, pp. 268–370, 1979. Note: a factor of 2 is missing in the square root of (4); the quantity 10.8 should read 20.8 in (12).
[28] J. R. Cozens and R. B. Dyott, "Higher-mode cutoff in elliptical dielectric waveguide," *Electron. Lett.*, vol. 15, pp. 558–559, 1979.
[29] In [26] and [28], the cut-off condition is based on the smaller core diameter rather than the larger diameter. This approach may allow multimode behavior in the long dimension.
[30] R. H. Stolen, V. Ramaswamy, P. Kaiser, and W. Pleibel, "Linear polarization in birefringent single-mode fibers," *Appl. Phys. Lett.*, vol. 33, pp. 699, 701, 1978.
[31] V. Ramaswamy, R. H. Stolen, M. D. Divino, and W. Pleibel, "Birefringence in elliptically clad borosilicate single-mode fibers," *Appl. Opt.*, vol. 18, pp. 4080–4084, 1979.
[32] V. Ramaswamy, W. G. French, and J. W. Shiever, "Borosilicate single polarization fibers," in *Tech. Dig. Integrated and Guided-Wave Conf.*, Include Village, NV, Paper MA5, Jan. 1980.
[33] V. Ramaswamy, I. P. Kaminow, P. Kaiser, and W. G. French, "Single polarization optical fibers: Exposed cladding technique," *Appl. Phys. Lett.*, vol. 33, pp. 814–816, 1978.
[34] I. P. Kaminow, J. R. Simpson, H. M. Presby, and J. B. MacChesney, "Strain birefringence in single-polarization germanosilicate optical fibers," *Electron. Lett.*, vol. 15, pp. 677–679, 1979.
[35] D. Marcuse, *Theory of Dielectric Optical Waveguides*. New York: Academic, 1974, ch. 5.
[36] D. Marcuse, "Coupled-mode theory for anisotropic optical waveguides," *Bell Syst. Tech. J.*, vol. 54, pp. 985–995, 1975.
[37] R. Ulrich, S. C. Rashleigh, and W. Eickhoff, "Bending induced birefringence in single-mode fibers," *Opt. Lett.*, vol. 5, pp. 273–275, 1980; S. C. Rashleigh and R. Ulrich, "High birefringence in tension-coiled single-mode fibers," *Opt. Lett.*, vol. 5, pp. 354–356, 1980.
[38] R. Ulrich and A. Simon, "Polarization optics of twisted single-mode fibers," *Appl. Opt.*, vol. 18, pp. 2241–2251, 1979; Yi Fujii and K. Sano, "Polarization coupling in twisted elliptical optical fiber," *Appl. Opt.*, vol. 19, pp. 2602–2605, 1980.
[39] Y. Namihira, M. Kudo, and Y. Mushiake, "Effect of mechanical stress on the transmission characteristics of optical fiber," *Trans. IECE* (Japan), vol. 60-C, pp. 107–115, 1977.
[40] R. E. Epworth, "The phenomenon of modal noise in fiber systems," presented at the Opt. Fiber Commun. Conf., Washington, DC, Mar. 1979, paper Th D1.
[41] H. Tsuchiya and N. Imoto, "Dispersion-free single-mode fibre in 1.5 μm wavelength region," *Electron. Lett.*, vol. 15, pp. 476–478, 1979.
[42] S. D. Personick, "Time dispersion in dielectric waveguide," *Bell Syst. Tech. J.*, vol. 50, pp. 843–859, 1971.
[43] H. Matsumura, T. Katsuyama, and T. Suganuma, "Fundamental study of single polansation fibres," presented at the 6th European Conf. Opt. Commun., York, England, Sept. 1980.

Ivan P. Kaminow (A'54–M'54–SM'73–F'74) received the B.S.E.E. degree from Union College, Schenectady, NY, the M.S.E. degree from the University of California, Los Angeles, and the Ph.D. degree in applied physics from Harvard University, Cambridge, MA. He was a Hughes Fellow at UCLA (1952–1954) and a Bell Laboratories CDTP Fellow at Harvard (1956–1960).

From 1952 to 1954 he worked on microwave antennas at Hughes Aircraft Company, Culver City, CA. Since 1954 he has been at Bell Laboratories, Holmdel, NJ, and has done research on antenna arrays, ferrite devices, electrooptic modulators, ferroelectrics, nonlinear optics, Raman scattering, integrated optics, semiconductor lasers, and optical fibers. He has been a Visiting Lecturer at Princeton University (1968), and at the University of California, Berkeley (1977). He is an Associate Editor of the IEEE JOURNAL OF QUANTUM ELECTRONICS and the author of *An Introduction to Electrooptic Devices* (1974).

Dr. Kaminow is a Fellow of the American Physical Society and the Optical Society of America.